HYDROGEN BRIDGING IN THE COMPOUNDS X_2H (X = AL, SI, P, S)

by

ZACHARY THOMAS OWENS

(Under the Direction of Henry F. Schaefer III)

ABSTRACT

X_2H hydrides (X=Al, Si, P, and S) have been investigated using coupled cluster theory with single, double, and triple excitations, the latter incorporated as a perturbative correction [CCSD(T)]. These were performed utilizing a series of correlation-consistent basis sets augmented with diffuse functions (aug-cc-pVXZ, X = D, T, Q). Al_2H and Si_2H are determined to have H-bridged C_{2v} structures in their ground states: the Al_2H ground state is of $^2B_1$ symmetry with an Al-H-Al angle of 87.6°, and the Si_2H ground state is of $^2A_1$ symmetry with a Si-H-Si angle of 79.8°. However, P_2H and S_2H have non-bridged, bent C_s structures: the P_2H ground state is of $^2A'$ symmetry with a P-P-H angle of 97.0°, and the S_2H ground state is of $^2A''$ symmetry with an S-S-H angle of 93.2°. Ground state geometries, vibrational frequencies, and electron affinities have been computed at all levels of theory.

INDEX WORDS: computational chemistry, coupled cluster, hydrogen bridging, quantum chemistry, Al2H, Si2H, P2H, S2H, electron affinities

HYDROGEN BRIDGING IN THE COMPOUNDS X_2H (X = AL, SI, P, S)

by

ZACHARY THOMAS OWENS

B. S., University of Toledo, 2002

A Thesis Submitted to the Graduate Faculty of The University of Georgia in Partial

Fulfillment of the Requirements for the Degree

MASTER OF SCIENCE

ATHENS, GEORGIA

2006

HYDROGEN BRIDGING IN THE COMPOUNDS X_2H (X = AL, SI, P, S)

by

ZACHARY THOMAS OWENS

Major Professor: Henry F. Schaefer III

Committee: Nigel A. Adams
Geoffrey D. Smith

Electronic Version Approved:

Maureen Grasso
Dean of the Graduate School
The University of Georgia
December 2006

TABLE OF CONTENTS

Page

LIST OF TABLES v

LIST OF FIGURES vi

CHAPTER

1 INTRODUCTION AND LITERATURE REVIEW 1

2 HYDROGEN BRIDGING IN THE COMPOUNDS X_2H (X = AL, SI, P, S) 4

2.1 ABSTRACT 5

2.2 INTRODUCTION 6

2.3 THEORETICAL METHODS 8

2.4 RESULTS 10

2.5 DISCUSSION 14

2.6 CONCLUSIONS 16

2.7 ACKNOWLEDGEMENTS 16

3 CONCLUDING REMARKS 27

REFERENCES 28

LIST OF TABLES

Page

TABLE 1: Relative energies (kcal/mol) and harmonic vibrational frequencies (cm^{-1}) for optimized geometries of Al_2H and Si_2H....................17

TABLE 2: Relative energies (kcal/mol) and harmonic vibrational frequencies (cm^{-1}) for the optimized geometries of P_2H and S_2H....................18

TABLE 3: Harmonic vibrational frequencies (cm^{-1}) for the optimized geometries of the Al_2H^-, Si_2H^-, P_2H^-, and S_2H^- anions....................19

TABLE 4: Adiabatic electron affinities (AEA) for Al_2H, Si_2H, P_2H, and S_2H in eV.. 20

TABLE 5: Dissociation energies of $X_2H \rightarrow X_2 + H$ (X = Al, Si, P, S) in kcal/mol....................21

LIST OF FIGURES

Page

FIGURE 1: Geometrical parameters of the $^{2}B_1$ Al_2H ground state and the $^{1}A_1$ Al_2H^- anion ground state. 22

FIGURE 2: Geometrical parameters of the $^{2}A_1$ Si_2H ground state and the $^{1}A_1$ Si_2H^- anion ground state geometries. 23

FIGURE 3: Geometrical parameters of the $^{2}A'$ P_2H ground state and the $^{1}A'$ P_2H^- anion ground state 24

FIGURE 4: Geometrical parameters of the $^{2}A''$ S_2H ground state and the $^{1}A'$ S_2H^- anion ground state. 25

FIGURE 5: Si_2H $^{2}A_1$ HOMO and P_2H $^{2}A'$ HOMO. 26

CHAPTER 1

INTRODUCTION AND LITERATURE REVIEW

Before the development of quantum mechanics, chemistry was largely an empirical science, where elements and compounds were categorized into groups and empirical rules about their properties determined. The underlying physical basis for these properties was unknown. Quantum mechanics changed that – most molecular behavior can now be understood from one concept, the solution to the Schrodinger equation.

Dirac once suggested that quantum mechanics changes chemistry into an exercise in applied mathematics. This is true in principle; however, in practice the exact solution to the Schrodinger equation is too difficult to compute for anything but the most trivial chemical systems. Much work has been done on the development of accurate and efficient approximations to the exact solution.

The first approximation made is the Born-Oppenheimer approximation. Since the nuclei in an atom are much heavier than the electrons, they move much more slowly. This allows us to assume that the electrons are moving in a fixed nuclear field, and the kinetic energy of the nuclei can be neglected. The repulsion between the nuclei is considered to be constant. The Born-Oppenheimer approximation lets us solve the electronic Schrodinger equation without worrying about the nuclei.

The electronic Schrodinger equation is still to computationally difficult to solve exactly, so a further approximation is made. In Hartree-Fock theory, the wavefunction is represented by a single determinant. Hartree-Fock recovers up to 99% of the total electronic energy of molecules. Unfortunately, that last bit is the part that determines a lot of the chemically interesting properties. *Ab initio* quantum chemistry methods are a series of corrections to the energy obtained in the Hartree-Fock approximation.

Inclusion of all possible determinants gives the Full Configuration Interaction (FCI) wavefunction. This is the exact non-relativistic energy within the Born Oppenheimer approximation. FCI can be practically computed only for very small systems. Between the HF and FCI extremes are a wide variety of different methods which utilize some subset of the determinants present in FCI. The 3 main families of methods are configuration interaction (CI), perturbation theory, and coupled cluster (CC) theory. Of these, the most accurate, robust, and efficient theory currently is coupled cluster. Like all *ab initio* methods, coupled cluster can currently only be applied to relatively small systems, but as computer power continues to increase, larger and larger systems can be treated with increasing accuracy.

There is another approach to solving the electronic Schrodinger equation that does not depend on explicitly computing the wavefunction like Hartree-Fock and all its refinements do. Density Functional Theory (DFT) is based on the fact that if the exact electron density is known, all the molecular properties can be derived from it. The problem with DFT is that the form of the exact functional is not known. Instead, approximate, parameterized functionals are used, which makes DFT only a semi-empirical method. The advantage of DFT is that its computations are very fast compared to *ab initio* methods, and for a wide variety of systems and properties it gives comparable results.

In the current work, coupled cluster theory including single and double excitations (CCSD) and coupled cluster including single and double excitations plus a perturbative triples contribution [CCSD(T)] are used to determine the properties of several molecules. DFT calculations are also done on these molecules in order to further determine its accuracy compared to coupled cluster methods.

CHAPTER 2

HYDROGEN BRIDGING IN THE COMPOUNDS X_2H (X = AL, SI, P, S)[†]

[†]Zachary T. Owens, Joseph D. Larkin, and Henry F. Schaefer III, *J. Chem. Phys*. **125**, 164322 (2006).

2.1 ABSTRACT

X_2H hydrides (X=Al, Si, P, and S) have been investigated using coupled cluster theory with single, double, and triple excitations, the latter incorporated as a perturbative correction [CCSD(T)]. These were performed utilizing a series of correlation-consistent basis sets augmented with diffuse functions (aug-cc-pVXZ, X = D, T, Q). Al_2H and Si_2H are determined to have H-bridged C_{2v} structures in their ground states: the Al_2H ground state is of $^2B_1$ symmetry with an Al-H-Al angle of 87.6°, and the Si_2H ground state is of $^2A_1$ symmetry with a Si-H-Si angle of 79.8°. However, P_2H and S_2H have non-bridged, bent C_s structures: the P_2H ground state is of $^2A'$ symmetry with a P-P-H angle of 97.0°, and the S_2H ground state is of $^2A''$ symmetry with an S-S-H angle of 93.2°. Ground state geometries, vibrational frequencies, and electron affinities have been computed at all levels of theory. Our CCSD(T)/aug-cc-pVQZ adiabatic electron affinity of 2.34 eV for the Si_2H radical is in excellent agreement with the photoelectron spectroscopy experiments of Xu, Taylor, Burton, and Neumark, where the electron affinity was determined to be 2.31 ± 0.01 eV.

2.2 INTRODUCTION

Silicon hydrides are relatively abundant species in Chemical Vapor Deposition (CVD) processes, primarily used in the semiconductor industry to produce thin silicon films.[1] In the high temperature plasmas created by this technique, silane (SiH_4) can be transformed[2] into isomers that include, among others, the disilaethynyl radical (Si_2H) and the disilaethynyl anion (Si_2H^-). The chemical properties of Si_2H predicted at reliable levels of theory should provide valuable insight into CVD experiments by identifying species that can prevent uniform layer deposition through the scavenging of reactant molecules.

Previously, theory has been used in the case of the valence isoelectronic species C_2H, which is known to have linear equilibrium geometries in its ground and first excited electronic states,[3] and Si_2H, which has been theoretically predicted to have a nonlinear, C_{2V} structure in its ground state.[4] It has been shown[5,6] that the difference in chemical properties of carbon and silicon compounds is due to the *s*- and *p*–like valence atomic orbitals of first row atoms being localized in roughly the same region of space, whereas for second and higher row, main group atoms the *s*- and *p*–like atomic orbitals are much more spatially separated. This causes single bonds between first-row elements to be weak and multiple bonds to be strong, while the opposite may be true for second and higher row elements.

While the above has been known for quite some time,[5,6] it provides impetus for understanding the electronic structure of second row hydrides, where the hydrogen bridge-bound C_{2V} geometries of the ground electronic states of Al_2H and Si_2H differ from the C_s symmetry structure of the P_2H and S_2H hydrides. The properties that are responsible for the unique bonding of these simple hydrides may help describe the more complex bonding environments of much larger clusters that have been the focus of considerable attention recently.[7-11] For example, binary clusters of silicon and hydrogen are thought to be present in hydrogenated amorphous silicon, porous silicon, and silicon surfaces, and their study may shed light on the complex phenomena occurring in these systems. Since second row clusters may become computationally prohibitive rather quickly as a function of cluster size, insight gained from high level theoretical studies of these smaller species is relevant.

Trans-phosphines, XP=PH, substituted with electron withdrawing substituents (X=F, Cl, OH, and NH_2), have been shown to have unusual bridged structures with angles less than 90°. Additionally, trans-phospine anions and cations can be readily formed via condensation reactions that combine phosphorus ions with phosphines.[12] These P_2H^- and P_2H^+ species also exhibit a similarly unique, bridged structure and have been investigated extensively with gas-phase ion chemistry techniques.[13] Theoretically, the neutral P_2H radical has been studied by Fueno and Akagi with MRD-CI methods,[14] predicting that the ground state of the P_2H radical ($^2A'$) is bent with a P-P-H angle of 99°. Interestingly, the first excited state of P_2H ($^2A_2$) is a bridged three π-electron system formed by the dehydrogenation of the lowest excited singlet state of HP=PH (^1B).[14]

S_2H was first detected in the flash photolysis of hydrogen sulfide,[15] and then later confirmed in the flash photolysis of hydrogen disulfide.[16] The spectrum was further studied by Gosavi, DeSorgo, Gunning, and Strausz,[17] who reported vibrational spacings of ~600 cm^{-1}, ~900 cm^{-1}, and ~2500 cm^{-1}, which were assigned to the S-S stretching, S-S-H bending, and S-H stretching modes, respectively. More recently, experiments by Holstein, Fink, Wildt, and Zabel[18] using chemiluminescence from electronically excited S_2H gave vibrational frequencies of 904 ± 8 cm^{-1} for the S-S-H bending mode and 595 ± 4 cm^{-1} for the S-S stretching mode. In

1999, Isoniemi, Khriachtchev, Pettersson, and Rasanen[19] isolated H_2S_2 in an argon matrix and produced S_2H by photolysis. Their infrared spectra showed S-H stretching modes of 2463 and 2460 cm^{-1} at different sites, and an S-S-H bending frequency of 903 $cm.^{-1}$ Theoretical studies of S_2H have also been performed,[20,21] most recently by Zhuo, Cloutier, and Goddard,[22] utilizing UMP2/6-31G(2d) computations that predict geometry and vibrational frequencies consistent with the above experimental results.

In the present study, CCSD(T) methods with a series of correlation consistent basis sets up to the aug-cc-pVQZ level have been used to reliably predict the ground state geometries and vibrational frequencies of the second row hydrides Al_2H, Si_2H, P_2H, and S_2H. In addition, since the negative ions of P_2H and Si_2H are known,[13] and analogous anions of Al_2H and S_2H are also suspected, the corresponding ground state anions will also be studied in order to determine the adiabatic electron affinities of these hydrides. Density functional theory computations were also performed to help calibrate our ongoing study of the use of DFT functionals with the DZP++ basis set for predicting electron affinities.[23]

2.3 THEORETICAL METHODS

All geometry optimizations and frequency analyses were carried out at the CCSD[24] and CCSD(T)[25,26] level of theory employing the Dunning-Woon[27,28] correlation-consistent polarized valence basis sets augmented with diffuse functions (aug-cc-pVDZ, aug-cc-pVTZ, and aug-cc-pVQZ). The largest basis set, aug-cc-pVQZ was contracted as follows: H(7*s*4*p*3*d*2*f*/5*s*4*p*3*d*2*f*), Al(17*s*12*p*4*d*3*f*2*g*/7*s*6*p*4*d*3*f*2*g*), Si(17*s*12*p*4*d*3*f*2*g*/7*s*6*p*4*d*3*f*2*g*), P(17*s*12*p*4*d*3*f*2*g*/7*s*6*p*4*d*3*f*2*g*), S(17*s*12*p*4*d*3*f*2*g*/7*s*6*p*4*d*3*f*2*g*). In these computations, the ten Hartree-Fock core molecular orbitals (1s-, 2s-, and 2p-like) on aluminum, silicon, phosphorus, and sulfur were frozen.

Computations were also carried out using the HF/DFT hybrid functional designated B3LYP, representing Becke's 3-parameter HF/DFT hybrid exchange functional (B3)[29] coupled with the dynamical correlation functional of Lee, Yang, and Parr (LYP).[30] Double-ζ quality basis sets with polarization and diffuse functions (DZP++) were used in these geometry optimizations and frequency analyses. The DZP++ basis sets were constructed from the Huzinaga-Dunning-Hay[31,32,33] sets of contracted Gaussian functions. A set of *p*-type polarization functions for each hydrogen atom was added, and one set of five *d*-type polarization functions was included on each heavy atom. These basis sets were further augmented with diffuse functions; a single s function for hydrogen, while each heavy atom received one additional *s*-type and one additional set of *p*-type functions. Each of these diffuse orbital exponents was determined in an even tempered sense according to the prescription set forth by Lee and Schaefer,[34]

$$\alpha_{diffuse} = \frac{1}{2}\left(\frac{\alpha_1}{\alpha_2} + \frac{\alpha_2}{\alpha_3}\right)\alpha_1$$

where α_1, α_2, and α_3 are the smallest Gaussian orbital exponents of the *s*- or *p*- type primitive functions for a given atom ($\alpha_1 < \alpha_2 < \alpha_3$) [$\alpha_s$(H) = 0.04415, α_s(Al) = 0.02148, α_p(Al) = 0.01891, α_s(Si) = 0.02729, α_p(Si) = 0.025, α_s(P) = 0.03448, α_p(P) = 0.03346, α_s(S) = 0.04267, α_p(S) = 0.04096]. The final contraction scheme for the smaller basis sets was as follows: H(5*s*1*p*/3*s*1*p*), Al(13*s*9*p*1*d*/7*s*5*p*1*d*), Si(13*s*9*p*1*d*/7*s*5*p*1*d*), P(13*s*9*p*1*d*/7*s*5*p*1*d*), S(13*s*9*p*1*d*/7*s*5*p*1*d*).

The forms of the neutral-anion energy difference reported are the adiabatic electron affinity, EA_{ad} = E(optimized neutral) – E(optimized anion), the vertical electron affinity, VEA = E(optimized neutral) – E(anion at neutral geometry), and the vertical detachment energy, VDE = E(neutral at anion geometry) – E(optimized anion).

DFT computations were carried out using the GAUSSIAN94[35] suite of programs, while the coupled cluster studies were performed with the MOLPRO[36] program package.

2.4 RESULTS

Optimized geometries of all species not included here are available in cartesian coordinate format in the supporting information.

A. Al_2H

Optimized geometries for the Al_2H radical are shown in Figure 1, where it may be seen that the ground state is predicted to be a hydrogen bridged $^2B_1$ structure. There also exists a low lying $^2A_1$ minimum predicted to lie only 0.18 kcal/mol higher [aug-cc-pVQZ CCSD(T)] in energy, and it is shown in Table 1S of the supporting information. The $^2B_1$ state is a more compact structure than the $^2A_1$ minimum, with an Al-Al bond 0.215 Å smaller than the $^2A_1$ state. Despite the significant geometry difference, these two states are nearly degenerate in energy at the aug-cc-pVQZ/CCSD(T) level.

B3LYP performs moderately well for predicting the ground state geometry of the $^2B_1$ C_{2v} isomer, differing from the CCSD(T) values by a very small 0.004 Å for the Al-H bond distance with a more significant change of 0.036 Å for the Al-Al bond, shown in Figure 1. B3LYP performs similarly for the $^2A_1$ isomer. In Table 1, the B3LYP energy separation of the two states is only 1.5 kcal/mol, where the $^2A_1$ state is predicted to be the ground state. This differs from the aug-cc-pVQZ/CCSD(T) energy gap by 1.7 kcal/mol and is not surprising considering that the energy separation between the two states is only 0.18 kcal/mol at the highest level of theory. This difference is outside of the expected accuracy range of DFT.[23,37]

The $^{1}A_1$ Al_2H^- ground state anion, shown in Figure 1, has a somewhat more compact structure than the neutral radical, with the Al-Al bond shortening by 0.050 Å and the Al-Al-H angle increasing by 0.85°, but it remains hydrogen bridged. Adding an electron to the Al_2H system stabilizes the radical, and the lower energy anion yields an adiabatic electron affinity of 1.11 eV at the aug-cc-pVQZ/CCSD(T) level of theory. The DZP++/B3LYP (0.95 eV), BHLYP (0.85 eV), and BLYP (0.83 eV) electron affinities differ from the CCSD(T) result; however, the BP86 method (1.11 eV) shows excellent agreement, see Table 4.

B. Si_2H

The optimized geometry for the ground state of the Si_2H radical is shown in Figure 2, and is an H-bridged $^{2}A_1$ structure, similar to the Al_2H system. Again, a low lying $^{2}B_1$ minimum is predicted to lie only 0.33 kcal/mol higher in energy than this ground state, and it is shown in the Supporting Information. In contrast to Al_2H, these two structures do not have a large geometry difference, with the $^{2}B_1$ state having an Si-Si bond length only 0.084 Å longer than the $^{2}A_1$ ground state. These two nearly degenerate states have been studied earlier[4,38-41] with an extensive variety of theoretical methods up to CCSDT, and our work is in good agreement with previous results of Pak *et al.*[4], who predicted the energy separation to be 0.37 kcal/mol at their most reliable level of theory, cc-pCVQZ CCSD(T). A vibrationally resolved photoelectron spectrum of Si_2H^- has been obtained by Xu, Taylor, Burton, and Neumark.[42] From their own *ab initio* computations, Neumark and coworkers predicted that photodetachment to the $^{2}A_1$ state results in a smaller geometry change than to the $^{2}B_1$ state, and assigned the ground state to be $^{2}A_1$. The experimental excitation energy $T_0(^{2}B_1)$ is 0.020 ± 0.005 eV, consistent with our theoretical result of 0.014 eV. We also find a linear Si_2H minimum – the $^{2}\Sigma^+$ state shown in

Table 1S of the Supporting Information and this isomer is 45.0 kcal/mol above the $^2A_1$ ground state. In addition, a linear $^2\Pi$ transition state, 9.3 kcal/mol above the ground state has been located.

B3LYP performs well in predicting the geometries of the C_{2v} Si_2H structures, with only small differences in bond lengths and angles (0.006 Å and 0.015 Å for the Si-Si bonds and 0.22° and 0.16° for the Si-Si-H angles), as may be seen in Figure 2 and Table 1S of the Supporting Information. However, the B3LYP DFT functional computes the wrong ground state for this molecule, predicting the $^2B_1$ state to be 0.97 kcal/mol lower in energy than the true ground state, $^2A_1$ giving an error of the energy splitting between the two states by 1.30 kcal/mol when compared to aug-cc-pVQZ/CCSD(T).

Adding an electron does not cause a large geometry change, as may be seen in the $^1A_1$ ground state Si_2H^- anion structure shown in Figure 2. The Si-Si bond shortens by 0.022 Å and the Si-Si-H angle decreases by 0.52°. Again, the extra electron stabilizes the radical, resulting in a computed adiabatic electron affinity of 2.34 eV at the aug-cc-pVQZ/CCSD(T) level of theory. The experimental electron affinity from Neumark[42] is 2.31 ± 0.01 eV, in excellent agreement with our results. In this case B3LYP also gives good agreement with the experimental electron affinity, with an AEA value of 2.31 eV. The other functionals do not perform as well, predicting the following electron affinities: BLYP 2.12 eV, BP86 2.38 eV, and BHLYP 2.20 eV.

C. P_2H

For the case of P_2H, we find that a hydrogen-bridged C_{2v} structure is no longer the ground electronic state. Instead, a bent $^2A'$ structure is predicted to be the global minimum shown in Figure 3. The lowest energy hydrogen bridged isomer was a $^2A_2$ state 28.3 kcal/mol above the bent ground state and is included in the Supporting Information. There also exists a $^2B_1$ transition state (Supporting Information) 87.1 kcal/mol above the $^2A'$ ground state. This is a transition state between the two bent structures where the hydrogen atom is transferred from one phosphorus atom to the other. Indeed, animation of the imaginary mode corresponds to this motion, confirming the hydrogen transfer, although no intrinsic reaction coordinate (IRC)[43] computations were performed. B3LYP predicts a similar geometry compared to coupled cluster theory for the $^2A'$ ground state (Figure 3).

The P_2H^- anion ($^1A_1$), shown in Figure 3, has a P-P-H bond angle 8.6° larger than that for the neutral radical, with P-P and the P-H bonds lengthening by 0.020 Å and 0.028 Å respectively. The adiabatic electron affinity is predicted to be 1.51 eV at the CCSD(T)/aug-cc-pVQZ level, with the B3LYP/DZP++ EA in very close agreement (1.53 eV) to CCSD(T). The BLYP, BP86, and BHLYP functionals predict adiabatic electron affinities of 1.38, 1.61, and 1.35 eV respectively.

D. S_2H

Our computations predict S_2H to have a bent geometry of $^2A''$ symmetry as the ground state minimum. This structure is shown in Figure 4, similar to P_2H, but having an X-X-H angle 4.3° larger. A bent C_s geometry of $^2A'$ symmetry was also located 19.9 kcal/mol higher in energy (Supporting Information). As may be seen from Figure 4, B3LYP predicts a similar geometry to CCSD(T) differing in S-S bond length by 0.03 Å and in bond angle by 0.9 degrees.

The computed adiabatic electron affinity at the CCSD(T)/aug-cc-pVQZ level is 1.93 eV and, as in the P_2H case, B3LYP with the DZP++ basis again predicts the AEA to be 0.02 eV larger. As with the above hydrides presented here, the other DFT functionals do not perform as well as B3LYP. Using BLYP, we obtained an adiabatic electron affinity of 1.77 eV; computations using BP86 result in 1.96 eV; and finally, the BHLYP functional gives an adiabatic electron affinity of 1.84 eV (Table 4). The geometry change in going from the S_2H^- anion, as shown in Figure 4, is not as large as that for the P_2H system. The S-S distance is longer in S_2H^- by 0.13 Å and the S-S-H bond angle is 0.1° larger.

2.5 DISCUSSION

The change in geometry from Si_2H to P_2H can be attributed to the bonding environment of the two heavy elements. Fueno and Akagi[14] illustrated the molecular orbital diagram for the first excited state of the P_2H radical and conclude from this that a stabilizing interaction occurs with the maximal overlap of the H-1s orbital and the P_2-π_u orbitals. Drawing our own inference from the molecular orbitals in their schematic, the occupation of the phosphorus dimer π_u orbitals determines whether or not these X_2H hydrides are hydrogen bridged. Incomplete occupation of the π_u orbitals in the Al_2H and Si_2H species maximizes the overlap of the H-1s orbital and the P_2-π_u orbitals favoring the hydrogen bridged structure as seen in the first excited state of the P_2H radical. This effect is also seen in the P_2H^+ cation and the $H_2P_2^+$ cation, having been demonstrated by Fueno and Akagi.[14] In the case of P_2H and S_2H, the diatomic π_u orbitals are fully occupied, strengthening the P-P and S-S bonds and thus weakening the hydrogen interaction with the two heavy elements. This nonbridged structure causes a weak H-P bond through the occupation of the H-1s orbital to a P_2-π_g^* anti-bonding orbital.

The above effect is illustrated in Figure 5, where the HOMOs of Si_2H and P_2H are plotted, showing the favorable bonding interaction in the case of Si_2H and the antibonding overlap in P_2H. Table 5 also demonstrates the strength of the H-X_2 bonds showing a minimum in the hydrogen dissociation energy for P_2H.

All four molecules have appreciably large and positive electron affinities. The trend across the period in electron affinities is consistent with the change in geometry at the Si-P divide. One sees an increase in EA from Al_2H to Si_2H as expected, and then a decrease to P_2H before rising again in the S_2H case. The decrease in electron affinity corresponds to the occupation of the π_g^* antibonding orbitals in the phosphorous and sulfer hydrides, destabilizing the anion.

Density functional theory, in particular the B3LYP functional paired with a DZP++ basis set, has proven to be an inexpensive and effective method of computing electron affinities.[23] For P_2H and S_2H, B3LYP predicted adiabatic electron affinities fall only 0.02 eV above the much more computationally demanding aug-cc-pVQZ/CCSD(T) level of theory. Al_2H and Si_2H both have a very low-lying excited electronic state, less that 0.5 kcal in energy above the ground state, and in these two cases B3LYP failed to predict the correct ground state for the neutral molecule. The BLYP and BHLYP functionals consistently underestimated the electron affinities compared to CCSD(T) while the BP86 overestimated the EAs in all cases. The magnitude of the errors for these three functionals varied for the different systems.

Only the Si_2H electron affinity has been determined experimentally, namely to be 2.31 ± 0.01 eV[42]; therefore direct comparisons with experimental data is limited. However, for Si_2H, the aug-cc-pVQZ/CCSD(T) method predicts an EA of 2.34 eV in very close agreement to the experimental value. As discussed previously, B3LYP determines the wrong ground state for this molecule but, when constrained to the correct electronic state, B3LYP predicted an adiabatic electron affinity of 2.31, a result fortuitously better than CCSD(T).

2.6 CONCLUSIONS

From high level structural studies of the X_2H hydrides (X=Al, Si, P, and S) we have demonstrated the Al_2H and Si_2H species to have H-bridged structures of C_{2v} symmetry as their ground electronic states while the P_2H and S_2H isomers were found to have bent structures of C_s symmetry. This interesting change in ground state geometry may be attributed to a favorable overlap of the aluminum and silicon π_u bonding orbitals with the hydrogen 1s orbital becoming unfavorable for the phosphorous and sulfur hydrides.

The B3LYP/DZP++ level of theory has again proven to be a rather robust method for computing electron affinities, comparing well to our most rigorous theoretical methods for these X_2H hydrides. In fact, B3LYP provided results for electron affinities nearly comparable in accuracy to the CCSD(T)/aug-cc-pVQZ method. The AEA at the CCSD(T)/aug-cc-pVQZ (B3LYP/DZP++) levels for Al_2H are predicted to be 1.11 eV (0.95 eV); for Si_2H the AEAs are 2.34 eV(2.31 eV); for P_2H the AEAs are 1.51 eV(1.53 eV); and for S_2H the AEAs are 1.93 eV(1.95 eV). With the exception of BP86 for Al_2H, the BLYP, BP86, and BHLYP functionals were not as successful as B3LYP in predicting adiabatic electron affinities.

2.7 ACKNOWLEDGEMENTS

The authors would like to sincerely thank the National Science Foundation for generous support under Grant CHE-0451445.

TABLE 1. Relative energies (kcal/mol) and harmonic vibrational frequencies (cm^{-1}) for optimized geometries of Al_2H and Si_2H.

Al_2H	Method	Energy	ω_1	ω_2	ω_3	ω_3
$^2B_1$	DZP++ B3LYP	1.5	1228	1015	259	
	aug-cc-pVQZ CCSD	1.6	1236	1050	278	
	aug-cc-pVQZ CCSD(T)	0.0	1242	1025	298	
$^2A_1$	DZP++ B3LYP	0.0	1075	996	218	
	aug-cc-pVQZ CCSD	0.0	1092	992	257	
	aug-cc-pVQZ CCSD(T)	0.2	1096	988	260	

Si_2H	Method	Energy	ω_1	ω_2	ω_3	ω_3
$^2A_1$	DZP++ B3LYP	1.0	1567	1090	544	
	aug-cc-pVQZ CCSD	2.1	1589	1166	555	
	aug-cc-pVQZ CCSD(T)	0.0	1574	1157	546	
	Experiment [Neumark[42]]		1592		540	
$^2B_1$	DZP++ B3LYP	0.0	1472	1012	512	
	aug-cc-pVQZ CCSD	0.0	1504	1057	548	
	aug-cc-pVQZ CCSD(T)	0.3	1490	1082	529	
	Experiment [Neumark[42]]		1491		520	
$^2\Pi$	DZP++ B3LYP	8.9	2183	569	49	40i
	aug-cc-pVQZ CCSD	10.4	2220	592	130	87i
	aug-cc-pVQZ CCSD(T)	9.3	2187	568	82	83i
$^2\Sigma^+$	aug-cc-pVQZ CCSD	48.3	2303	719	446	446
	aug-cc-pVQZ CCSD(T)	45.0	2263	683	354	354

TABLE 2. Relative energies (kcal/mol) and harmonic vibrational frequencies (cm^{-1}) for the optimized geometries of P_2H and S_2H.

P_2H	Method	Energy	ω_1	ω_2	ω_3	ω_3
$^2A'$	DZP++ B3LYP	0.0	2264	673	604	
	aug-cc-pVQZ CCSD	0.0	2336	682	639	
	aug-cc-pVQZ CCSD(T)	0.0	2305	663	610	
$^2A_2$	aug-cc-pVQZ CCSD	28.5	1773	660	1057	
	aug-cc-pVQZ CCSD(T)	28.3	1751	635	1100	
$^2\Pi$	aug-cc-pVQZ CCSD	42.9	2563	711	202i	1501i
	aug-cc-pVQZ CCSD(T)	40.4	2522	685	205i	1508i
$^2B_1$	aug-cc-pVQZ CCSD	88.6	1720	470	1554i	
	aug-cc-pVQZ CCSD(T)	87.1	1674	454	1591i	

S_2H	Method	Energy	ω_1	ω_2	ω_3	ω_3
$^2A''$	DZP++ B3LYP	0.0	2554	910	559	
	aug-cc-pVQZ CCSD	0.0	2647	933	603	
	aug-cc-pVQZ CCSD(T)	0.0	2608	921	599	
	Experiment [Isoniemi[19]]		2463	903		
	Experiment [Holstein[18]]			904	595	
$^2A'$	aug-cc-pVQZ CCSD	18.9	2706	794	517	
	aug-cc-pVQZ CCSD(T)	19.9	2674	769	505	
	Experiment [Holstein[18]]				504	
$^2\Pi$	DZP++ B3LYP	70.2	2748	504	1395i	1718i
	aug-cc-pVQZ CCSD	73.4	2797	582	1458i	1810i
	aug-cc-pVQZ CCSD(T)	71.1	2758	566	1425i	1789i

TABLE 3. Harmonic vibrational frequencies (cm^{-1}) for the optimized geometries of the Al_2H^-, Si_2H^-, P_2H^-, and S_2H^- anions.

	Method	ω_1	ω_2	ω_3
Al_2H^-	DZP++ B3LYP	1213	1028	292
	aug-cc-pVQZ CCSD	1225	1077	311
	aug-cc-pVQZ CCSD(T)	1223	1042	325
Si_2H^-	DZP++ B3LYP	1487	1081	557
	aug-cc-pVQZ CCSD	1521	1147	582
	aug-cc-pVQZ CCSD(T)	1508	1172	558
P_2H^-	DZP++ B3LYP	1988	824	587
	aug-cc-pVQZ CCSD	2097	831	619
	aug-cc-pVQZ CCSD(T)	2050	812	597
S_2H^-	DZP++ B3LYP	2542	808	415
	aug-cc-pVQZ CCSD	2638	839	488
	aug-cc-pVQZ CCSD(T)	2599	822	478

TABLE 4. Adiabatic electron affinities (AEA) for Al_2H, Si_2H, P_2H, and S_2H in eV.

	AEA (eV)	VEA (eV)	VDE (eV)
$^2B_1 \rightarrow {}^1A_1$ Transition			
Al_2H DZP++ B3LYP	0.95	0.94	0.96
Al_2H DZP++ BLYP	0.83	0.82	0.84
Al_2H DZP++ BP86	1.11	1.10	1.12
Al_2H DZP++ BHLYP	0.85	0.75	0.88
Al_2H aug-cc-pVQZ CCSD	0.96	0.95	0.97
Al_2H aug-cc-pVQZ CCSD(T)	1.11	1.10	1.38
$^2A_1 \rightarrow {}^1A_1$ Transition			
Si_2H DZP++ B3LYP	2.31	2.30	2.31
Si_2H DZP++ BLYP	2.12	2.12	2.13
Si_2H DZP++ BP86	2.38	2.37	2.39
Si_2H DZP++ BHLYP	2.20	2.20	2.20
Si_2H aug-cc-pVQZ CCSD	2.28	2.28	2.29
Si_2H aug-cc-pVQZ CCSD(T)	2.34	2.34	2.34
Experiment [Neumark[41]]	2.31		
$^2A' \rightarrow {}^1A'$ Transition			
P_2H DZP++ B3LYP	1.53	1.46	1.58
P_2H DZP++ BLYP	1.38	1.32	1.44
P_2H DZP++ BP86	1.61	1.54	1.66
P_2H DZP++ BHLYP	1.35	1.29	1.40
P_2H aug-cc-pVQZ CCSD	1.43	1.37	1.48
P_2H aug-cc-pVQZ CCSD(T)	1.51	1.44	1.56
$^2A'' \rightarrow {}^1A'$ Transition			
S_2H DZP++ B3LYP	1.95	1.81	2.11
S_2H DZP++ BLYP	1.77	1.63	1.92
S_2H DZP++ BP86	1.96	1.83	2.10
S_2H DZP++ BHLYP	1.84	1.69	1.99
S_2H aug-cc-pVQZ CCSD	1.88	1.74	2.73
S_2H aug-cc-pVQZ CCSD(T)	1.93	1.79	2.83

TABLE 5. Dissociation energies of $X_2H \rightarrow X_2 + H$ (X = Al, Si, P, S) in kcal/mol.

	Dissociation Energy
Al_2H aug-cc-pVQZ CCSD(T)	81.5
Si_2H aug-cc-pVQZ CCSD(T)	88.2
P_2H aug-cc-pVQZ CCSD(T)	36.9
S_2H aug-cc-pVQZ CCSD(T)	77.4

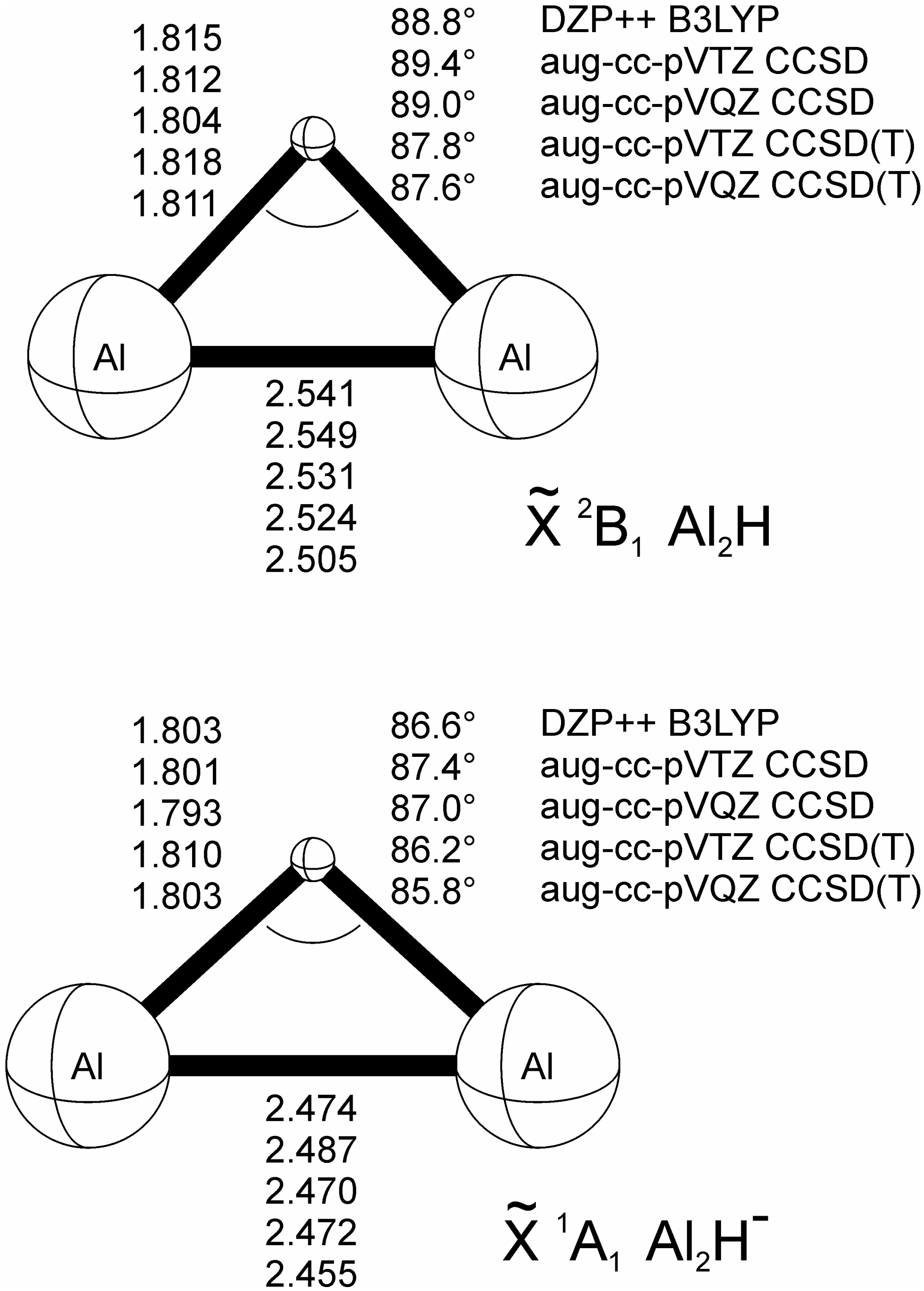

FIGURE 1. Geometrical parameters of the $^2B_1$ Al_2H ground state and the $^1A_1$ Al_2H^- anion ground state.

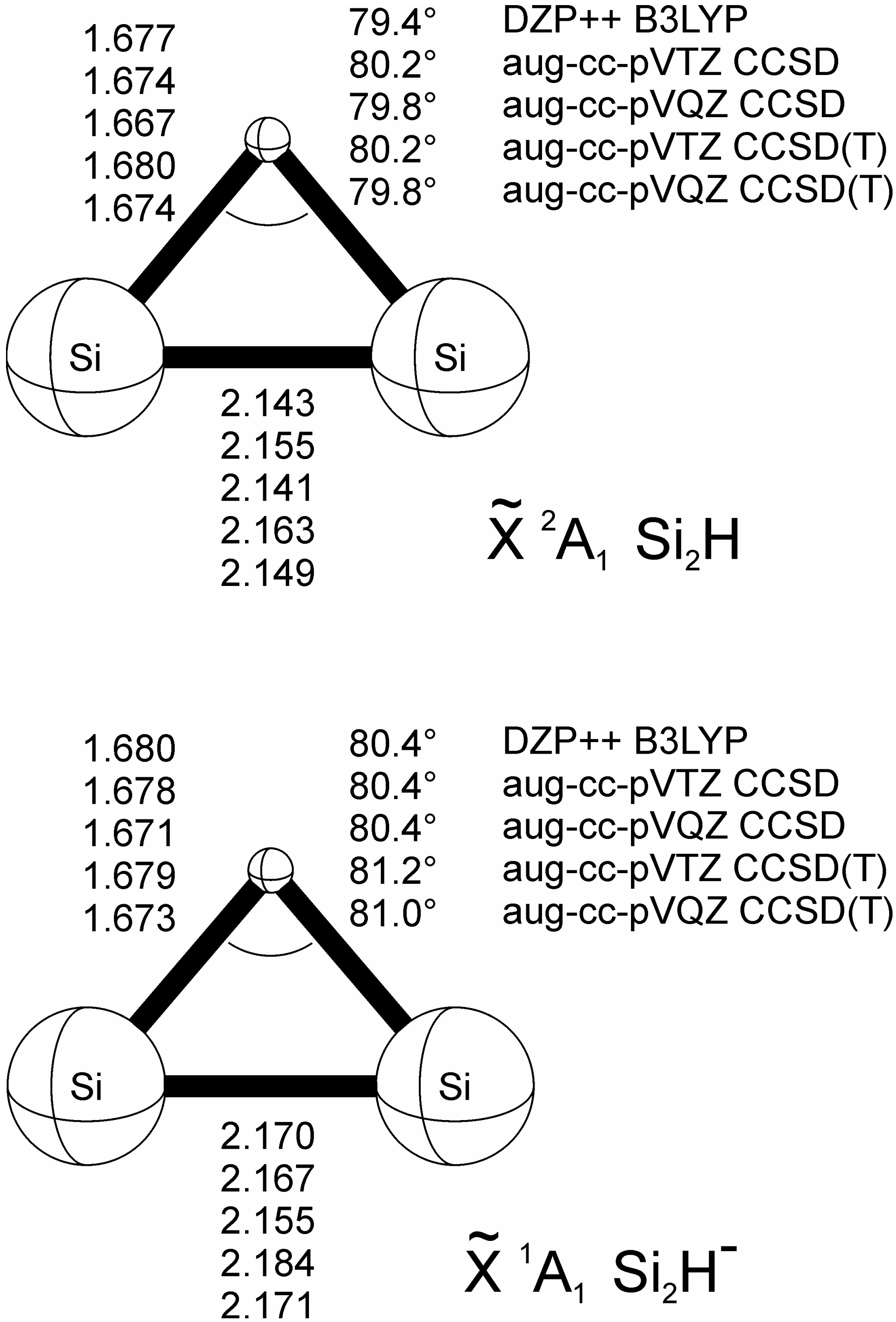

FIGURE 2. Geometrical parameters of the $^2A_1$ Si_2H ground state and the $^1A_1$ Si_2H^- anion ground state geometries.

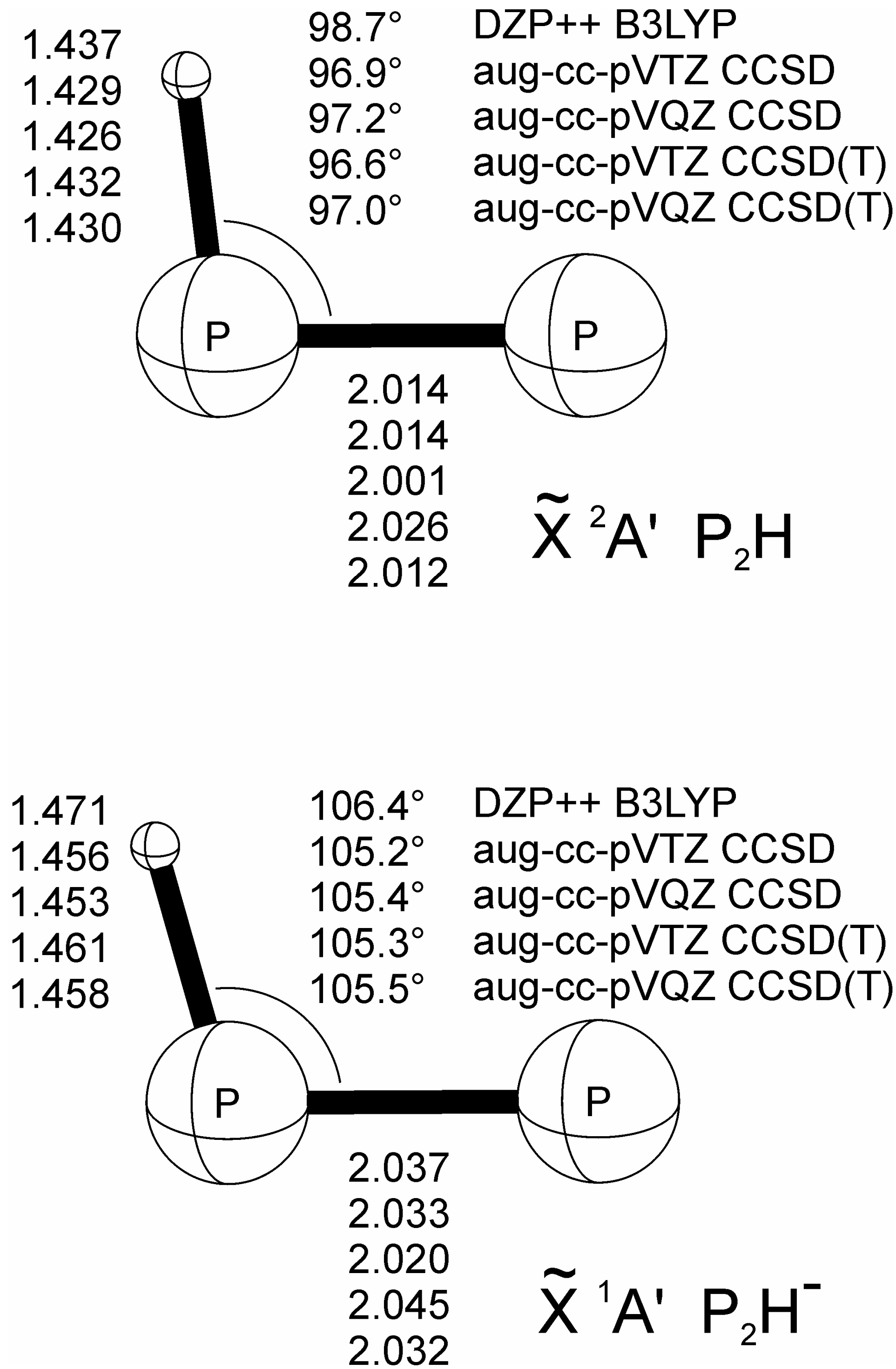

FIGURE 3. Geometrical parameters of the $^2A'$ P_2H ground state and the $^1A'$ P_2H^- anion ground state.

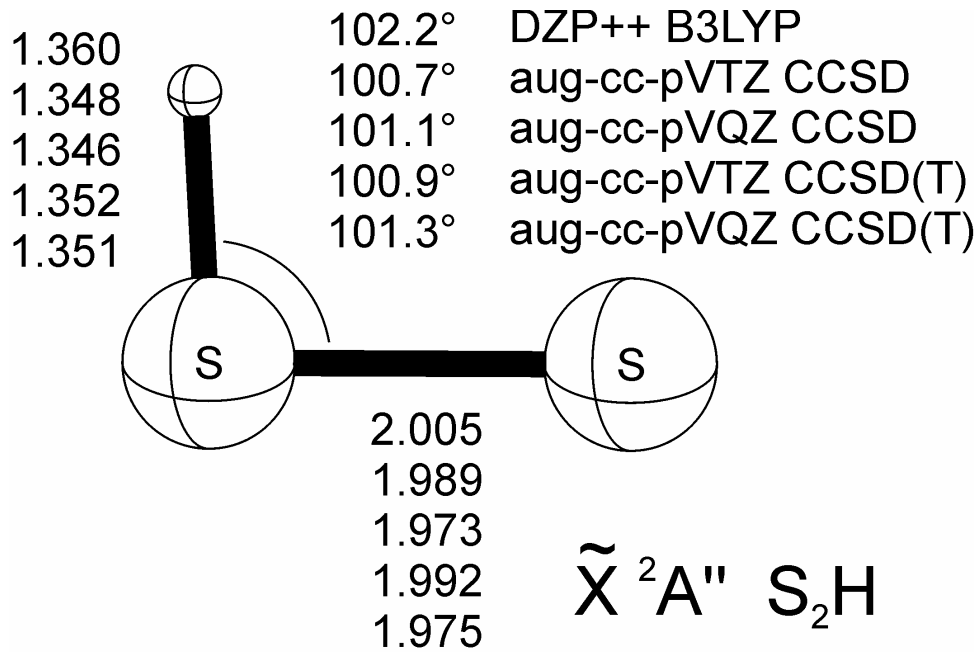

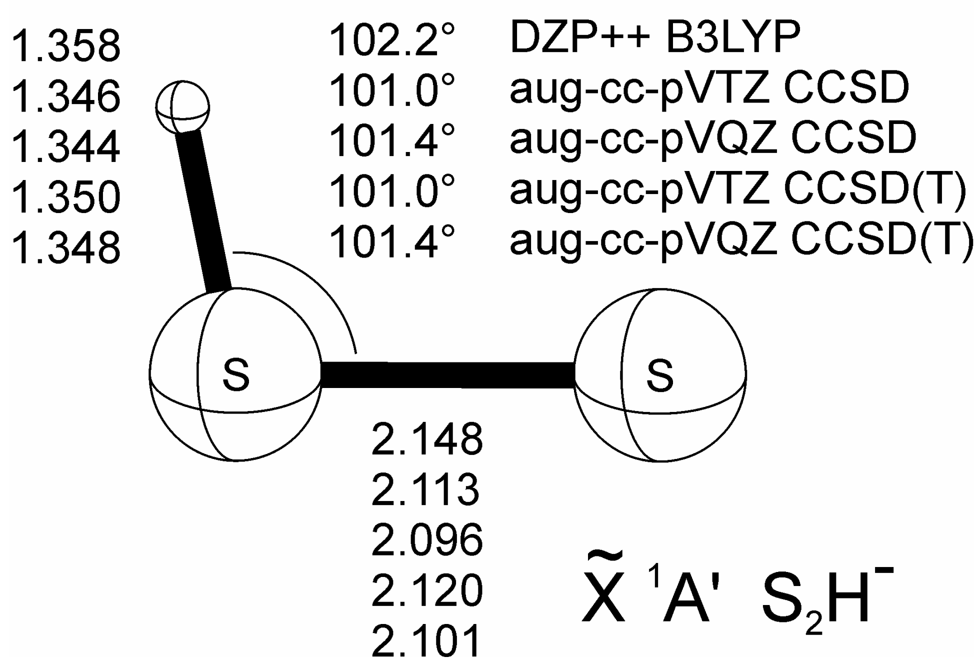

FIGURE 4. Geometrical parameters of the $^2A''$ S_2H ground state and the $^1A'$ S_2H^- anion ground state.

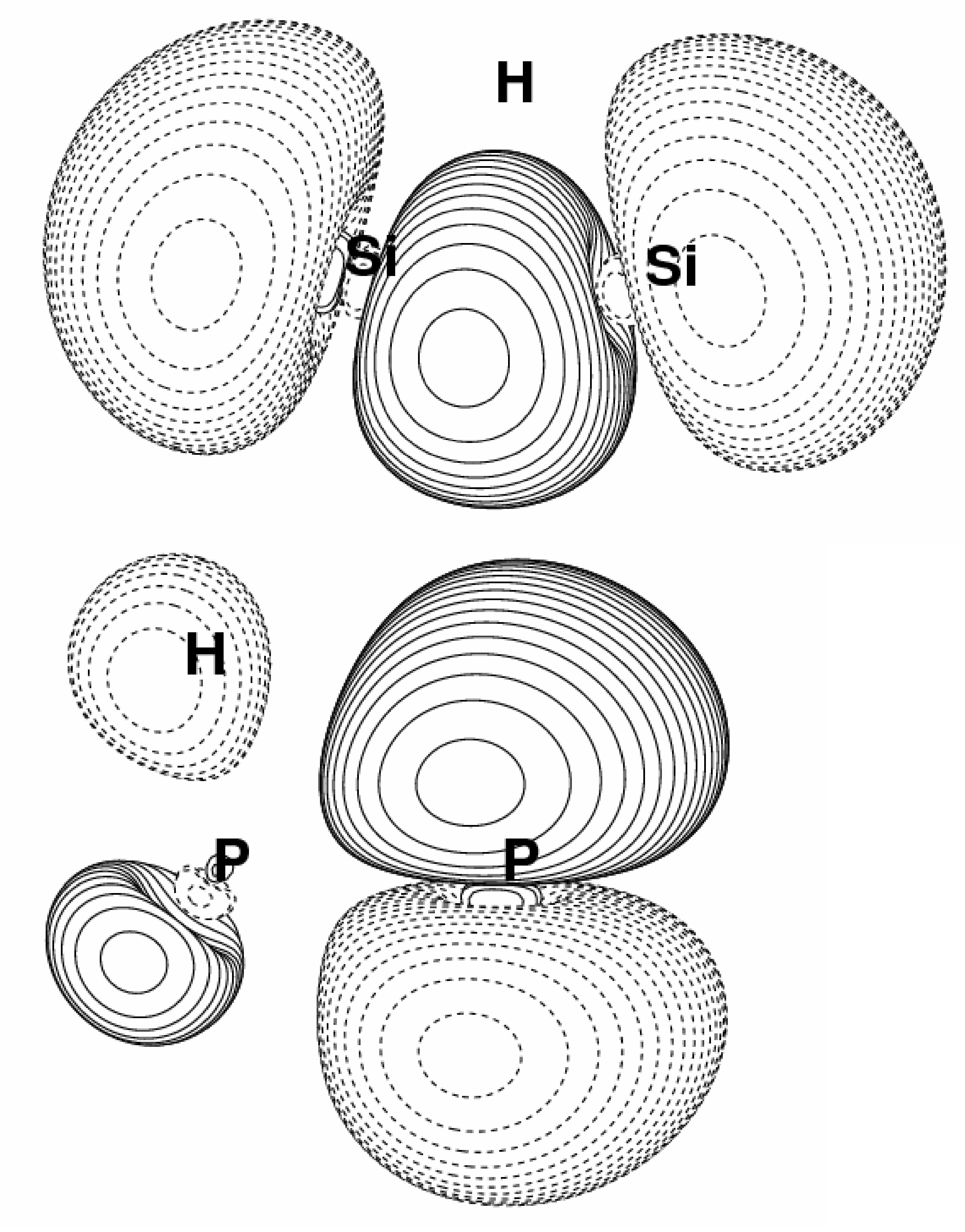

FIGURE 5. Si_2H $^2A_1$ HOMO and P_2H $^2A'$ HOMO.

CHAPTER 3

CONCLUDING REMARKS

Ab initio theory has once again provided useful insight into the properties of molecules which have not been studied extensively by experiment. Accurate theoretical properties are not only useful in themselves, but can help guide future experimental work on these and related systems.

From high level structural studies of the X_2H hydrides (X=Al, Si, P, and S) it has been demonstrated that the Al_2H and Si_2H species have H-bridged structures of C_{2v} symmetry as their ground electronic states while the P_2H and S_2H isomers were found to have bent structures of C_s symmetry. This interesting change in ground state geometry may be attributed to a favorable overlap of the aluminum and silicon π_u bonding orbitals with the hydrogen 1s orbital becoming unfavorable for the phosphorous and sulfur hydrides.

The B3LYP/DZP++ level of theory has again proven to be a rather robust method for computing electron affinities, comparing well to our most rigorous theoretical methods for these X_2H hydrides. In fact, B3LYP provided results for electron affinities nearly comparable in accuracy to the CCSD(T)/aug-cc-pVQZ method. The AEA at the CCSD(T)/aug-cc-pVQZ (B3LYP/DZP++) levels for Al_2H are predicted to be 1.11 eV (0.95 eV); for Si_2H the AEAs are 2.34 eV(2.31 eV); for P_2H the AEAs are 1.51 eV(1.53 eV); and for S_2H the AEAs are 1.93 eV(1.95 eV). With the exception of BP86 for Al_2H, the BLYP, BP86, and BHLYP functionals were not as successful as B3LYP in predicting adiabatic electron affinities.

REFERENCES

[1] R. L. Puurunen, J. Appl. Phys. **97**, 121301 (2005).

[2] J. M. Jasinski, B. S. Meyerson, and B. A. Scott, Ann. Rev. Phys. Chem. **38**, 109 (1987).

[3] A. Largo and C. Barrientos, J. Chem. Phys. **138**, 291 (1989).

[4] C. Pak, S. S. Wesolowski, J. C. Rienstra-Kiracofe, Y. Yamaguchi, and H. F. Schaefer, J. Chem. Phys. **115**, 2157 (2001).

[5] W. Kutzelnigg, Angew. Chem. Int. Ed. Engl. **22**, 272 (1984).

[6] W. Kutzelnigg, J. Mol. Struct. **169**, 403 (1988).

[7] D. Balamurugan and R. Prasad, Phys. Rev. B **64**, 205406 (2001).

[8] R. Prasad and S. R. Shenoy, Phys. Lett. A **218**, 85 (1996).

[9] F. Buda, G. L. Chiarotti, R. Car, and M. Parrinello, Physica B **170**, 98 (1991).

[10] S. B. Zhang and H. M. Branz, Phys. Rev. Lett. **84**, 967 (2000).

[11] B. Tuttle, C. G. Van de Walle, and J. B. Adams, Phys. Rev. B **59**, 5493 (1999).

[12] D. Holtz, J. L. Beauchamp, and J. R. Eyler, J. Am. Chem. Soc. **92**, 7045 (1970).

[13] R. A. J. O'Hair, M. Krempp, R. Damrauer, and C. H. DePuy, Inorg. Chem. **31**, 2092 (1992).

[14] T. Fueno and H. Akagi, Theor. Chim. Acta **92**, 1 (1995).

[15] G. Porter, Discuss. Faraday Soc. **9**, 60 (1950).

[16] O. P. Strausz, R. J. Donovan, and M. Desorgo, Ber. Bunsenges. Physik. Chem. **72**, 253 (1968).

[17] R. K. Gosavi, M. DeSorgo, H. E. Gunning, and O. P. Strausz, Chem. Phys. Lett. **21**, 318 (1973).

[18] K. J. Holstein, E. H. Fink, J. Wildt, and F. Zabel, Chem. Phys. Lett. **113**, 1 (1984).

[19] E. Isoniemi, L. Khriachtchev, M. Pettersson, and M. Rasanen, Chem. Phys. Lett. **311**, 47 (1999).

[20] A. B. Sannigrahi, S. D. Peyerimhoff, and R. J. Buenker, Chem. Phys. Lett. **46**, 415 (1977).

[21] A. B. Sannigrahi, J. Mol. Struct. **44**, 223 (1978).

[22] Q. Zhou, D. J. Clouthier, and J. D. Goddard, J. Chem. Phys. **100**, 2924 (1993).

[23] J. C. Rienstra-Kiracofe, G. S. Tschumper, H. F. Schaefer, S. Nandi, and G. B. Ellison, Chem. Rev. **102**, 231 (2002).

[24] G. D. Purvis and R. J. Bartlett, J. Chem. Phys. **76**, 1595 (1982).

[25] K. Raghavachari, G. W. Trucks, J. A. Pople, and M. Head-Gordon, Chem. Phys. Lett. **157**, 479 (1989).

[26] G. E. Scuseria, Chem. Phys. Lett. **176**, 27 (1991).

[27] T. H. Dunning, J. Chem. Phys. **90**, 1007 (1989).

[28] D. E. Woon and T. H. Dunning, J. Chem. Phys. **89**, 1358 (1993).

[29] A. D. Becke, J. Chem. Phys. **98**, 5648 (1993).

[30] C. Lee, W. Yang, and R. G. Parr, Phys. Rev. B **37**, 785 (1988).

[31] T. H. Dunning and P. J. Hay, Modern Theoretical Chemistry **3**, 1 (1977).

[32] S. Huzinaga, J. Chem. Phys. **42**, 1293 (1965).

[33] S. Huzinaga, *Approximate Atomic Wavefunctions II* (University of Alberta, 1971).

[34] T. J. Lee and H. F. Schaefer, J. Chem. Phys. **83**, 1784 (1985).

[35] M. J. Frisch, G. W. Trucks, and H. B. Schlegel et al., GAUSSIAN 94, Revision E.2 (Gaussian Inc., Pittsburg, PA, 1995).

[36] H. J. Werner and P. J. Knowles et al., MOLPRO, Version 2002.6 (2003).

[37] W. Koch and M. C. Holthausen, *A Chemist's Guide to Density Functional Theory* (Wiley-VCH, 2001).

[38] B. Ma and N. L. Allinger, J. Chem. Phys. **105**, 5731 (1996).

[39] L. A. Curtiss, K. Raghavachari, P. W. Deutsch, and J. A. Pople, J. Chem. Phys. **95**, 2433 (1991).

[40] J. Kalcher and A. F. Sax, Chem. Phys. Lett. **215**, 601 (1993).

[41] C. Pak, L. Sari, J. C. Rienstra-Kiracofe, S. S. Wesolowski, L. Horny, Y. Yamaguchi, and H. F. Schaefer, J. Chem. Phys. **118**, 7256 (2003).

[42] C. Xu, T. R. Taylor, G. R. Burton, and D. M. Neumark, J. Chem. Phys. **108**, 7645 (1998).

[43] K. Fukui, J. Phys. Chem. **74**, 4161 (1970).